

Method of Correction of Longitudinal Chromatic Aberrations

Oleg Konevsky

Optical Systems Division, Image Sensor Modules Team

Samsung Electro-Mechanics Co. Ltd., Suwon, South Korea

oleg.konevsky@samsung.com

Abstract

Inexpensive lenses, in particular the lenses used in compact consumer digital cameras, often suffer from a large amount of longitudinal chromatic aberrations (LCA). LCA affect the image quality in two ways: reduce the sharpness, and produce color fringing around high-contrast edges. The image processing method described in this paper can be used to reduce or eliminate the effect of LCA. We use the sharpness estimation technique in order to generate correction mask, which is applied to the original image. Parameter-free algorithm enables LCA correction without sensor noise amplification.

Keywords: *longitudinal chromatic aberrations, sharpness enhancement, blur estimation, correction mask.*

1. INTRODUCTION

Refractive index of optical materials depends on the wavelength of the transmitted light. This results in splitting of the white light into the spectrum, when the beam is transmitted through the prism. Another example of visualization of this phenomenon is longitudinal chromatic aberrations. This effect can be seen on a number of digital or film photographs shot with the budget lenses, especially if the contrast of the scene is relatively high.

Due to longitudinal chromatic aberrations (LCA) the light beam composed of different wavelengths cannot be focused in a single plane. The beams of shorter wavelengths (blue region of the visible spectrum) focus closer to the lens, while the beams of longer wavelengths (red) – farther from the lens. It means that depending on the position of the imager with respect to the lens only a portion of the original light beam focuses on the sensor plane. The remaining portion of light incidents the imager being defocused. As soon as the middle part of the spectrum (green region of visible spectrum) contributes most into overall sharpness of the image, the imager is typically placed into the position, where the beams of middle wavelengths focus, allowing some defocus in shorter and longer wavelengths (Fig. 1a).

LCA cause image quality deterioration in two ways. On the one hand, defocus of two color channels of three causes degradation of overall MTF (Fig. 1b). On the other hand, due to the different blur in color channels, there is an insufficient light intensity on one side and excessive intensity on the other side of high-contrast edge in some of the color channels. It results in color artifacts around high-contrast edges, commonly referred to as color fringing (Fig. 1c).

Inexpensive lenses, especially the ones used in budget consumer cameras or the built-in camera modules for the cell phones and other mobile devices, usually suffer from large amount of LCA. Even though optical methods of chromatic correction are well known and widely applied to the design of professional lenses

(achromatic and apochromatic designs), these techniques are of limited use for budget lenses and mobile device lenses, because they cause dramatic increase of cost and/or total track length of the optical system. Moreover, with the constantly improving semiconductor technologies, and due to the chase of manufacturers for miniaturization and cost efficiency, the pixel pitch of sensors is shrinking by 25% from one generation to the next. This makes the cameras that feature modern imagers be more sensitive to LCA than ever. Therefore there is a need for digital image processing method enabling to eliminate the effect of LCA for inexpensive slim lenses.

On the other hand, there are techniques, which allow taking some advantages out of large LCA. One of them is proposed in [1]. The sharpness difference between the color channels is used to reduce the number of focusing steps of the optical system with passive auto-focusing. In another work [2], a method of deriving spatial depth information from LCA is described. Full use of these techniques can be made only if the amount of aberrations is significant. But it is unlikely that one will find the artifacts caused by LCA to be an acceptable price for these advanced features of the camera in consumer photography. Therefore, the images taken with such a device also should also be subject to LCA correction.

A method of correction of longitudinal chromatic aberrations is proposed in [3]. The method is easy to implement in both software and hardware, and based on high-pass filtering of blurred color channels, thus improving their sharpness. However this approach has some weaknesses which make it unpractical. First, high-pass filter while amplifying high frequencies of the signal, amplifies the sensor noise as well.

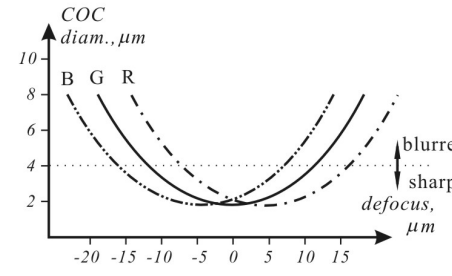
Second, the blur difference between the color channels depends on focusing. This is especially significant for fixed focus cameras, because the best focusing cannot be guaranteed. But even if the camera is equipped with auto-focusing mechanism, the scene typically has some spatial depth; therefore some objects still may appear out of the best focusing position. Thus, the blur difference between the color channels, and consequently the amount of sharpness enhancement required, may vary depending on the distance from the camera to the object and focusing situation.

It can be seen on the spot diagram in the Fig. 1a. For example, for the object located at the best focusing distance from the camera (defocus is close to 0 μm), the difference between the circle-of-confusion (COC) diameters in green and blue color channels is about 0.5 μm , while for the object at shorter distance with defocus, let us say -10 μm , the difference between COC diameters is about 2 μm . Obviously, a single high pass filter cannot be used to compensate such differing blurs, filter kernel has to be adjusted for each case individually. Therefore, the mentioned above method cannot be considered as fully automatic.

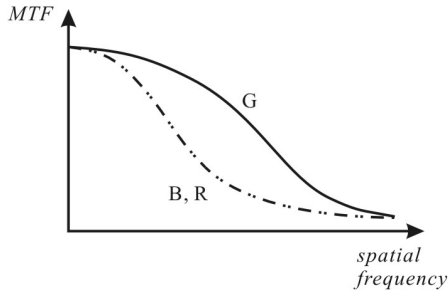
Another method of LCA correction is claimed in [4], however no details of the algorithm are disclosed. It is clear, however, that the method is based on some sort of “sharpness transfer” from one color channel to another.

We describe a new parameter-free method of LCA correction in this paper. According to the proposed method, the correction is concentrated around the reliable edges only. As soon as SNR is measured on uniform areas of the images, it is not altered by the correction. On the other hand, the method has adaptability to the blur difference between color channels, which makes it suitable for LCA correction regardless of the shooting distance even for fixed focus cameras.

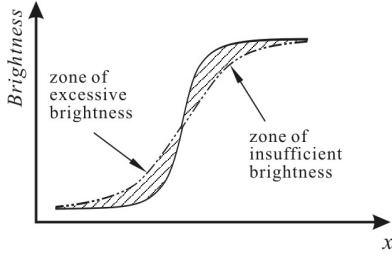
In our following discussion, we will assume that the imager is equipped with color filter array, composed of the elements sensitive to green (G) and blue (B) colors. The elements sensitive to the similar wavelengths compose color channel. The beams of middle portion of the spectrum, which correspond to



(a)



(b)



(c)

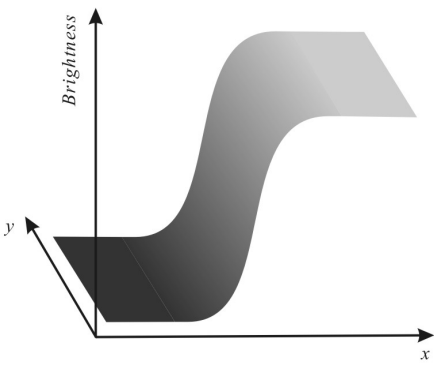
Figure 1: An example of spot diagram (a) and MTF graph (b). Note the degradation of MTF in blue and red color channels. The zones of color fringing around the high-contrast edge are shown on the edge profile (c).

the green color channel, focus in the point located at the imager plane. That means, the image in green color channel has the highest sharpness and the least blur. The image in blue color channels appears more blurred because of LCA effect. Even though in most practical cases the imager’s color filter array actually contains three color channels (red, green and blue), everything stated throughout this paper regarding green-blue correction holds with no change for the couple green-red.

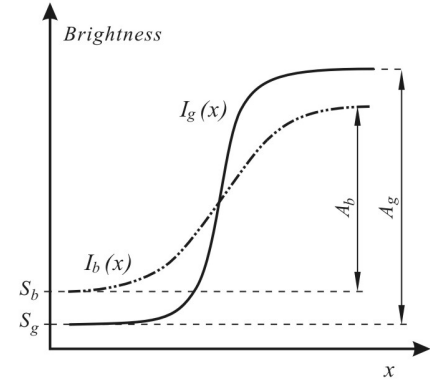
2. GENERAL APPROACH AND THEORY

2.1 Assumptions and notation

Let us consider the image projected by the lens that has significant longitudinal chromatic aberrations. The original image is shown in the Fig. 2a, and represents a step edge – transition from the dark uniform area to the bright one. For the sake of simplicity, we align the coordinate system in such a way, that the edge direction is perpendicular to one of the axes, for instance y . Thus, we will be able to eliminate variable y from the formulas, in spite of two-dimensional nature of the signal.



(a)



(b)

Figure 2: Original image: transition from dark to bright region (a); the profile of the image, registered by the sensor (b). In general, the magnitude of the edge is different in different color channels; blur is also different due to the effect of LCA.

Due to LCA, the image in each color channel is blurred to a different extent. Let us assume the lens is adjusted to focus light in the middle portion of the visible spectrum (green channel) as close to the imager plane as possible. Then, the image in blue color channel will be more blurred, than in green one. The edge profile captured by the sensor in green and red color channels after the original image is transmitted through the lens is shown in the Fig. 2b. Denote the edge profile in green and blue color channels as $I_g(x)$ and $I_b(x)$ respectively. Let the magnitude of the step edge be A_g in green and A_b – in blue color channel, the brightness pedestal – S_g and S_b respectively.

2.2 LCA correction: graphic approach

In order to correct LCA, we need to change the edge profile in blue color channel in such a way, that the blur in both color channels would be equivalent. That means, the edge profiles after correction, being normalized by the step edge magnitude, should coincide. Therefore, the shape of correction mask can be determined as follows. First, we normalize the edges in each color channel by magnitude and remove the corresponding pedestals S_g and S_b :

$$\bar{I}_g(x) = (I_g(x) - S_g)/A_g \quad (1.1)$$

$$\bar{I}_b(x) = (I_b(x) - S_b)/A_b \quad (1.2)$$

Then, subtracting the normalized edge profile in green color channel from the one in blue color channel, we obtain normalized correction mask $\bar{M}(x)$ (Fig. 3a):

$$\bar{M}(x) = \bar{I}_b(x) - \bar{I}_g(x) \quad (2)$$

As soon as the correction mask is supposed to alter the edge profile in blue color channel, its normalized counterpart is scaled by the corresponding step edge magnitude (Fig. 3b):

$$M(x) = \bar{M}(x) \cdot A_b = (\bar{I}_b(x) - \bar{I}_g(x)) \cdot A_b \quad (3)$$

Now we can add correction mask values to the corresponding image pixel values in blue color channel, to get corrected image (Fig. 3c):

$$I_b^{cor}(x) = I_b(x) + M(x) \quad (4)$$

Note, the magnitude of the original step edge and pedestal in blue color channel remain unaltered, while the blur amount becomes the same as in green color channel.

2.3 LCA correction: analytical approach

Let us obtain analytical equations and the algorithm for correction mask profile calculation. As we have mentioned before, the correction mask is nothing but the difference between the two normalized step edge profiles, scaled with the magnitude of the step edge in blue color channel. Let us represent each of two normalized step edges $\bar{I}_g(x)$ and $\bar{I}_b(x)$ as a convolution product of the unit step edge $E(x)$ with some filter kernel. Note that two main factors contribute into the edge blur observed in the imager plane: natural blur (penumbral blur, shading, etc.) $F^{(nat)}$ and focal blur of the optical system $F_g^{(focal)}, F_b^{(focal)}$:

$$E(x) = \begin{cases} 0 & \text{for } x < x_0 \\ 1 & \text{for } x \geq x_0 \end{cases} \quad (4)$$

$$\bar{I}_g = E * F^{(nat)} * F_g^{(focal)} \quad (5.1)$$

$$\bar{I}_b = E * F^{(nat)} * F_b^{(focal)} \quad (5.2)$$

In most of real-world scenarios natural blur $F^{(nat)}$ is the same for all the color channels, while focal blur differs due to longitudinal chromatic aberrations.

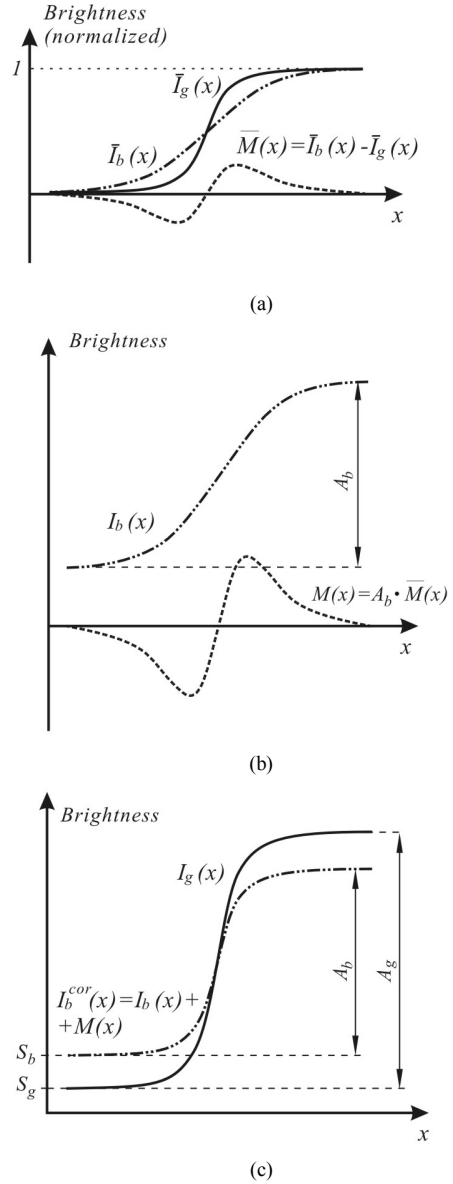


Figure 3: Normalized correction mask, defined as a difference between the normalized edge profiles (a); correction mask as its normalized version scaled with the magnitude of step edge in blue color channel (b); edge profile after correction: the values of correction mask are added to the brightness values in blue color channel.

As it is shown in [5], in most of the cases, natural blur can be expressed in terms of Gaussian low-pass filter. At the same time, focal blur in the diffraction limited optical system can be approximated by convolution with Gaussian filter kernel. That means, both $F^{(nat)}(x)$ and $F^{(focal)}(x)$ are Gaussian curves. As soon as the product of convolution of two Gaussians is a Gaussian, we can replace natural and focal blur with one filter kernel, individual for each color channel [6]:

$$G_g = F^{(nat)} * F_g^{(focal)} \quad (6.1)$$

$$G_b = F^{(nat)} * F_b^{(focal)} \quad (6.2)$$

Thus, substituting natural and focal blur in (5.1) and (5.2) with Gaussians, and taking into account convolution properties, we obtain the equations for normalized edge profiles:

$$\bar{I}_g(x) = \int G_g(x) E(x) dx \quad (7.1)$$

$$\bar{I}_b(x) = \int G_b(x) E(x) dx, \quad (7.2)$$

where:

$$G_g(x) = \frac{1}{2\pi\sigma_g^2} \exp\left(\frac{-(x^2 + \mu^2)}{2\sigma_g^2}\right) \quad (8.1)$$

$$G_b(x) = \frac{1}{2\pi\sigma_b^2} \exp\left(\frac{-(x^2 + \mu^2)}{2\sigma_b^2}\right) \quad (8.2)$$

Note, that Gaussians $G_g(x)$ and $G_b(x)$ have unit integral, because we assume that both natural blur and focal blur of the optical system do not change the overall light energy.

After substitution of $\bar{I}_g(x)$ and $\bar{I}_b(x)$ in (7.1) and (7.2) with (8.1) and (8.2) respectively, the expression for calculation of the correction mask will be:

$$\begin{aligned} M(x) &= A_b \int G_b(x) E(x) - G_g(x) E(x) dx = \\ &= A_b \int (G_b(x) - G_g(x)) E(x) dx \end{aligned} \quad (9)$$

There are the following unknowns in (9): step edge magnitude in green color channel A_b , dispersion σ_g^2 of the Gaussian G_g , dispersion σ_b^2 of the Gaussian G_b , and the position of the maximum of the Gaussian curve μ . Note, that σ_g^2 and σ_b^2 essentially represent the blur measure, including natural and focal blur.

The unknowns are to be calculated based on the image registered by the sensor. We applied a modified method, described in [6].

In order to evaluate blur parameters and edge magnitude, we produce a gradient image for each color channel $I'_g(x)$ and $I'_b(x)$ respectively. A Gaussian low-pass filter with the kernel $G(x; \hat{\sigma}^2)$ is applied to the original image prior to the gradient operator to reduce the sensitivity to the sensor noise:

$$I'_g = (I_g * G(\hat{\sigma}^2))' \quad (10.1)$$

$$I'_b = (I_b * G(\hat{\sigma}^2))' \quad (10.2)$$

$$G(x; \hat{\sigma}^2) = \frac{1}{2\pi\hat{\sigma}^2} \exp\left(\frac{-x^2}{2\hat{\sigma}^2}\right) \quad (11)$$

The dispersion of the Gaussian $\hat{\sigma}^2$ is referred to as a filter scale. Taking into account the properties of convolution's derivative, we can rewrite (10.1) and (10.2) in the following form:

$$I'_g = I_g * G'(\hat{\sigma}^2), \quad (12.1)$$

$$I'_b = I_b * G'(\hat{\sigma}^2), \quad (12.2)$$

where the first derivative of Gaussian or Gaussian derivative filter kernel is [7, 8]:

$$G'(x; \hat{\sigma}^2) = \frac{-x}{2\pi\hat{\sigma}^4} \exp\left(\frac{-x^2}{2\hat{\sigma}^2}\right) \quad (13)$$

If our assumption regarding the form of natural and focal blur holds, the edge profile on the gradient image will be a Gaussian curve.

Let us determine the values of functions $I'_g(x)$ and $I'_b(x)$ in three points to define the shape of Gaussian curve. Even though these points may be chosen arbitrarily, selecting them near the peak of the curve will result in higher precision of the calculations. For the same reason and due to the discrete nature of the image, the points should correspond to the adjacent pixels of the image (Fig. 4). That is, when selecting the points, we follow the rules:

1. point p_2 is located between the points p_1 and p_3 , i.e. $p_2 \in (p_1, p_3)$;
2. the distance between the points p_1 and p_2 , and points p_2 and p_3 is the same and equals to one, i.e. $|p_1 - p_2| = |p_2 - p_3| = 1$;
3. p_2 is located not farther away from the point, corresponding to the maximum of the gradient function, than the other two points, i.e.:

$$I'_g(p_2) \geq I'_g(p_1)$$

$$I'_g(p_2) \geq I'_g(p_3)$$

$$I'_b(p_2) \geq I'_b(p_1)$$

$$I'_b(p_2) \geq I'_b(p_3)$$

Thus, we have the system of three equations for each color:

$$\begin{cases} I'_g(p_1) = A_g \exp\left(\frac{p_1^2 - \mu^2}{\sigma_g^2 + \hat{\sigma}^2}\right) \\ I'_g(p_2) = A_g \exp\left(\frac{p_2^2 - \mu^2}{\sigma_g^2 + \hat{\sigma}^2}\right). \\ I'_g(p_3) = A_g \exp\left(\frac{p_3^2 - \mu^2}{\sigma_g^2 + \hat{\sigma}^2}\right) \end{cases} \quad (14.1)$$

$$\begin{cases} I'_b(p_1) = A_b \exp\left(\frac{p_1^2 - \mu^2}{\sigma_b^2 + \hat{\sigma}^2}\right) \\ I'_b(p_2) = A_b \exp\left(\frac{p_2^2 - \mu^2}{\sigma_b^2 + \hat{\sigma}^2}\right). \\ I'_b(p_3) = A_b \exp\left(\frac{p_3^2 - \mu^2}{\sigma_b^2 + \hat{\sigma}^2}\right) \end{cases} \quad (14.2)$$

Having solved (14) with respect to blur parameters σ_g^2 and σ_b^2 , step edge magnitude A_b and the position of the maximum of the Gaussian curve μ , needed for the proper positioning of the correction mask on the image, we obtain the following formulas:

$$Q = \frac{\ln(I'_{g1}) - \ln(I'_{g2})}{\ln(I'_{g1}) - \ln(I'_{g3})} \quad (15)$$

$$\mu = \frac{1}{4Q - 2} \quad (16)$$

$$\sigma_g^2 = \frac{-4\mu}{\sqrt{2} \ln\left(\frac{I'_{g1}}{I'_{g3}}\right)} - \hat{\sigma}^2 \quad (17.1)$$

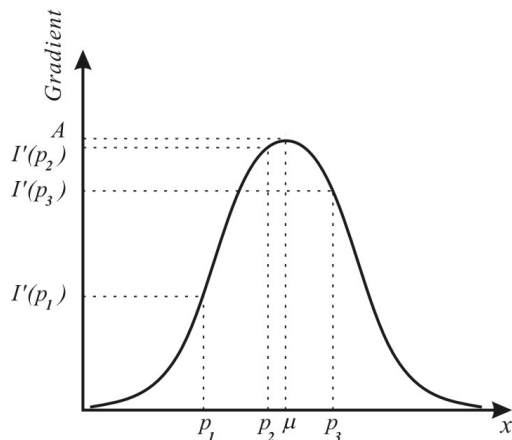


Figure 4: Profile of gradient image and location of points used for the edge parameters calculation.

$$\sigma_b^2 = \frac{-4\mu}{\sqrt{2} \ln\left(\frac{I'_{b1}}{I'_{b3}}\right)} - \hat{\sigma}^2 \quad (17.2)$$

$$A_b = \frac{I'_{b2}}{K \cdot \exp\left(-\frac{\mu^2}{2(\sigma_b^2 + \hat{\sigma}^2)}\right)} \quad (18)$$

where K is the coefficient, calculated as a result of convolution of a unit step edge $E(x)$, Gaussian with the dispersion σ_b^2 , and derivative of the Gaussian with dispersion $\hat{\sigma}^2$ in the point $x = 0$:

$$K = E * G(\sigma_b^2) * G'(\hat{\sigma}^2)|_{x=0} \quad (19)$$

The coefficient represents the ratio of the Gaussian curve's maximum, obtained as a result of transform of the original edge profile, to the initial step edge magnitude.

We assume that the shift of the Gaussian curve's maximum with respect to the point p_2 is the same for both green and blue color channels. If the assumption does not hold, the parameters Q and μ should be calculated individually for each color channel using corresponding values. In this case, mask is to be positioned with the shift obtained for blue color channel.

Thus, all the unknowns, required for the calculation of the correction mask profile, have been found.

The correction mask is applied to the image in blue color channels: it is positioned in the point μ , its values are added to the corresponding values of the image. As a result of the correction, according to (4), the blur in blue color channel becomes equivalent to the blur in green color channel, i.e. the effect of longitudinal chromatic aberrations is eliminated.

3. IMPLEMENTATION

In this section we describe the implementation of LCA correction algorithm. As soon as the processing is essentially the same in vertical and horizontal directions, we will consider the correction in one direction only.

First, the image in green and blue color channels is filtered with one-dimensional Gaussian derivative filter, to obtain the gradient images. Our experiments with the filters of different scales showed that the optimal combination of filter sensitivity to the weak edges and stability against sensor noise is achieved with the filter scale $\hat{\sigma} = 0.5$. Moreover, with the selected scale, the filter kernel is quite compact and consists of as few as three significant elements: $\{-0.35, 0, 0.35\}$, which is advantageous especially for real-time applications.

Then, the peaks on the gradient image in green color channel and corresponding peaks in blue color channel are searched for. Only the peaks with the magnitude higher than the threshold are taken into account. The threshold value is calculated with the formula proposed in [6]

$$T(\hat{\sigma}^2) = \frac{1.1s_n}{\hat{\sigma}^2} \quad (20)$$

where s_n – is the dispersion of the sensor noise.

The peaks on the gradient with the lower magnitude are considered to be unreliable, i.e. they could be caused merely as a result of sensor noise, and do not represent any discontinuities of real surfaces. Therefore, these peaks are ignored.

For each peak, the parameters of the edges σ_g^2 , σ_b^2 , A_b , μ are calculated using (15) – (18). Point p_2 is a point corresponding to the local maximum of the gradient, p_1 and p_3 – points next to p_2 on the sides from it.

The values of coefficient K are stored in one-dimensional look up table. Note, that in (19) one of two variables, namely $\hat{\sigma}^2$, is set in advance, therefore we can precalculate the values of the look up table for K as a function of σ_b^2 only. This enables to reduce the amount of calculation during the process of correction. Then, the values of correction mask are calculated using (8.1), (8.2), and (9), taking into account shift μ . In our implementation, we used correction mask composed of eight elements. The elements out of this range are likely to be always zero for the optical system with reasonable amount of aberrations. However, in many practical cases the mask of as few as six elements was found to be suitable for high-quality correction.

As soon as a pixel of the image experiences the influence of light distributed from many edges, not necessarily aligned along the coordinate axes, the correction mask values are accumulated for each particular pixel. Upon the completion of the calculation, accumulated correction value is added to the pixel value.

4. RESULTS

We have tested the LCA correction algorithm on 2M pixel fixed focus camera module for mobile phones. We used three different lenses: one of them showed mild level of LCA, second – moderate level and third one – severe LCA. Focusing was made at the recommended distance of 1.2 m. Raw Bayer image acquired from the module was fed to the LCA correction program. The result of correction was also in the form of raw Bayer image, which was processed by means of commercial image signal processor (ISP). ISP included the following functions: dead pixel correction, lens shading correction, noise reduction, interpolation, color enhancement, contrast enhancement, edge enhancement, bitmap format conversion. Also, the original raw image was processed by means of the same ISP to obtain the reference image for the comparison and evaluation. In both cases edge enhancement function was turned off.

ISO resolution chart was used for the quantitative evaluation of the results. Slanted edge was shot at different distances to cover different focusing situations from close-up to hyper focal distance

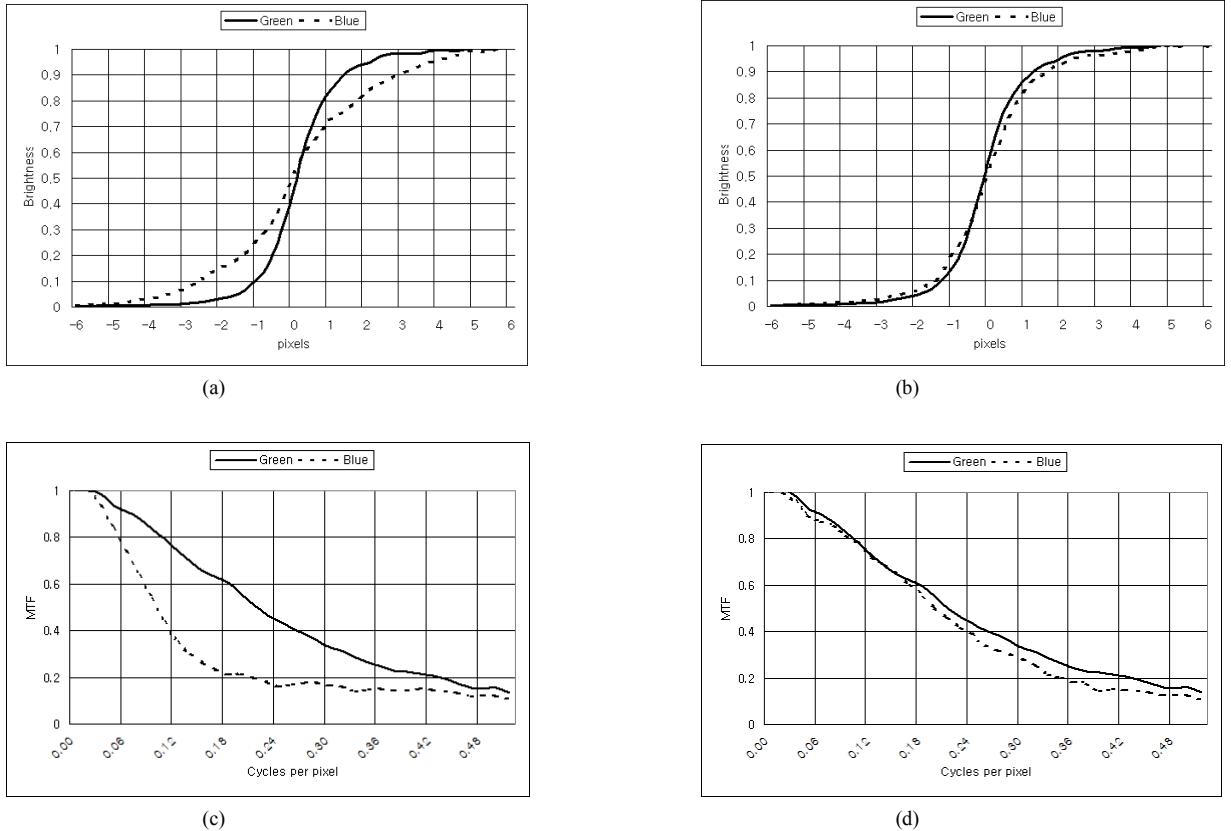


Figure 5: Slanted edge on the ISO resolution chart: edge profile before (a) and after (b) correction; MTF graph before (c) and after (d) correction.

Table 1: B-G difference in 10-90% brightness rise, pix

Lens #	Before/after LCA correction	Shooting distance, cm				
		60	90	120	180	250
1	before	-1.7	-0.2	0.3	0.8	1.6
	after	-0.7	-0.2	0.1	0.2	0.4
2	before	-2.2	0.0	0.7	1.5	3.5
	after	-0.8	0.1	0.4	0.4	0.5
3	before	-2.5	-0.2	1.2	3.1	5.3
	after	-0.9	-0.3	0.2	0.8	1.2

(250 cm can be considered a hyper focal for these lenses). Then, we measured MTF value according to ISO methodology before and after LCA correction. In order to compare the blur amount in different color channels, we used the number of pixels covered by 10-90% rise of the brightness near the edge. Strictly speaking, this is not equivalent to the diameter of circle of confusion of the optical system; however the value reflects the change of the edge profile caused by the correction, therefore suits our task.

An example of edge profile and corresponding MTF curves before and after LCA correction are shown in the Fig. 5. One can observe the rise of MTF in the middle spatial frequencies in blue color channel, as well as caused by it insignificant rise of overall MTF. The edge profile after correction is almost collinear with one in green color channel. This is also reflected in 10-90% rise of brightness area in blue color channel (reduced from 5.5 pix to about 2.9 pix).

The results of our experiments with the three lenses are shown in the Table 1. Here, negative B-G difference means, that blue spot size is smaller, than green spot size. This is usually the case in close-up shooting conditions. LCA correction blurs blue color channel to achieve the same blur amount as in green channel. Obviously, the increase of MTF for blue color channel cannot be expected in this situation. But still this complies with the concept of LCA correction: blur in reference channel (green) and corrected channel (blue) should be equivalent.

For all three lenses LCA algorithm demonstrated the ability to correct LCA. In the case of Lens 1 the correction amount was rather small, just enough to eliminate mild aberrations. In the case of Lens 2, in spite of larger amount of LCA, the correction was as good as for Lens 1. However, for the Lens 3 some residual aberrations still remained after correction, especially at hyper focal distances, where the blur difference between the color channels is the largest. The reason of that lies in ability of Gaussian derivative filter to detect edges with the large blur. In some cases the filter fails to detect all the peaks on the edge, thus increasing the probability of undercorrection. Also, the precision of edge parameters' calculation degrades significantly, because quantization error of brightness becomes comparable to the difference between the gradient values in the neighborhood of point P_2 .

A number of experiments showed, reliable (with no visible residual color artifacts and MTF deterioration) LCA correction is achieved with the proposed method, if the difference between COC diameters in different color channel is not larger, than four pixels.

5. CONCLUSION

We have described the method of correction of longitudinal chromatic aberrations in this paper. The effect of LCA is eliminated by means of digital image processing. This allows releasing the constraints to optical design, which in turn enables to design the lenses with special properties: slim lenses, optical systems with extended depth of field, larger aperture, low-cost, etc.

6. REFERENCES

- [1] A. Ning, *Auto-focus (AF) Lens and Process*. US Patent application 10/778,785.
- [2] J. Garcia, J.M. Sanchez, X. Orrilos, X. Binefa, *Chromatic Aberration and Depth Extraction*. Proc. of 15-th International Conference on Pattern Recognition (ICPR'00), p. 1762 (2000).
- [3] J. Bescos, I. Glaser, A.A. Sawchuk, *Restoration of color images degraded by chromatic aberrations*. Applied Optics, 19, 3869 (1980).
- [4] L. Chanas et al. *Method of Controlling an Action, such as Sharpness Modification, using a Colour Digital Image*. Patent application PCT/FR2006/050197.
- [5] J. S. Elder, *The Visual Computation of Bounding Contours*, PhD thesis, McGil University, 1995.
- [6] J.S. Elder, S.W. Zucker, *Local Scale Control for Edge Detection and Blur Estimation*. IEEE Transactions on Pattern Analysis and Machine Intelligence, 20, 699 (1998).
- [7] W. Freeman, E. Andelson, *The Design and Use of Steerable Filters*. IEEE Transactions on Pattern Analysis and Machine Intelligence, 13, 891 (1991).
- [8] P. Perona, *Deformable kernels for early vision*. IEEE Transactions on Pattern Analysis and Machine Intelligence, 17, 488 (1995).

About the author

Oleg Konevsky received M.E. degree from Novgorod State University in 1995, and Ph.D. degree from St. Petersburg State Polytechnic University in 1998. Since 2005, he has been a Principal Engineer at Samsung Electro-Mechanics Co., Ltd, Optical Systems Division. His professional interests include image enhancement, pattern recognition, digital still cameras, and video cameras for automotive applications.